Durability testing of solar receiver coatings: Experimental results for T91 and VM12 substrates

Cite as: AIP Conference Proceedings **2303**, 150006 (2020); https://doi.org/10.1063/5.0028772
Published Online: 11 December 2020

Simon Caron, Yaniv Binyamin, Mubeen Baidossi, Alina Agüero, Christina Hildebrandt, Mathias Galetz, and Florian Sutter

Durability Testing of Solar Receiver Coatings: Experimental Results for T91 and VM12 Substrates

Simon Caron[1,a)], Yaniv Binyamin[2], Mubeen Baidossi[2], Alina Agüero[3], Christina Hildebrandt[4], Mathias Galetz[5], Florian Sutter[1]

[1]*German Aerospace Center (DLR), Institute of Solar Research, Plataforma Solar de Almería (PSA), Carretera de Senes km.5 , 04200 Tabernas, Spain*
[2]*Brightsource Industries, 11 Kiryat Mada St., Amot bldg. 6, P.O. Box 45220, Har Hotzvim, Jerusalem, 91450 Israel*
[3]*Instituto Nacional de Tecnica Aerospacial (INTA), Ctra. De Ajalvir km.4, 28850 Torrejón de Ardoz, Spain*
[4]*Fraunhofer Institut für Solare Energiesysteme (ISE), Heidenhofstr. 2, 79110 Freiburg, Germany*
[5]*DECHEMA-Forschungsinstitut, Theodor-Heuss-Allee 25, 60486 Frankfurt am Main, Germany*

[a)] Corresponding author: simon.caron@dlr.de

Abstract. In Central Receiver Systems, the receiver coating absorbs the concentrated sunlight from the heliostat field and needs to withstand high thermal stresses in harsh desert climates. Coating degradation is associated to high repair and down-time costs and therefore several research activities have been conducted in the past years to increase the service lifetime of receiver coatings. This paper presents the durability test results of six novel receiver coatings developed for operation temperatures of 600°C. The coatings were deposited on ferritic-martensitic steel coupons made of T91 and VM12-SHC. The testing program involved a sequential accelerated aging test: on-sun testing with an average flux level of 300 kW/m² was combined with isothermal furnace testing and humidity testing at low temperature to mimic condensation on the receiver during night-time. In addition, climate chamber tests have been carried out. This paper summarizes test results and identifies the most promising coating developments.

INTRODUCTION

Receiver coating degradation is associated to expensive recoating procedures: the aged coating needs to be removed from the receiver tubes by sand blasting and afterwards the damaged panel section needs to be recoated and cured. In the worst case, receiver panels have to be dismounted and the recoating process takes place in a workshop on the ground. This entire procedure is associated to high maintenance and down-time costs. For these reasons, a high coating durability is essential for the profitability of solar thermal tower plants.

The development and testing of solar receiver coatings for solar thermal tower plants is an active research field. Pyromark 2500 [1] has long been considered as the state of the art coating. The influence of its application parameters on the coating durability has been recently investigated [2]. Alternative receiver coatings formulations have also been published [3,4,5]. The challenge is to develop a receiver coating with a High Solar Absorptance (HSA), with proven durability at a high temperature, typically above 600 °C at a minimal Levelized Cost of Coating (LCOC) [6,7]. Durability testing for such coatings is not yet standardized, different test procedures combining isothermal testing and cyclic thermal loads with muffle furnaces have been proposed [7,8,9]. However, most of the reported tests did not include on-sun testing with concentrated solar radiation.

Within the European project Raiselife [10], a first generation of high temperature solar receiver coatings has been tested previously under concentrated solar radiation [11, 12]. These receiver coatings, also referred as absorber coatings, are designed to improve the opto-thermal efficiency of external tube receivers mounted in Central Receiver Systems (CRS), operating with steam or molten salts as a Heat Transfer Fluid (HTF) [13].

SolarPACES 2019
AIP Conf. Proc. 2303, 150006-1–150006-10; https://doi.org/10.1063/5.0028772
Published by AIP Publishing. 978-0-7354-4037-1/$30.00

This paper reports experimental results of durability testing for a second generation (Gen2) of receiver coatings, optimized after metallurgical analysis of the first generation (Gen1), in order to improve opto-thermal efficiency and durability. Six coating formulations are compared, including two Solar Selective Coatings (SSC) formulations. These coatings are applied on ferritic-martensitic steels T91 (X10CrMoVNb9-1) [14] and VM12-SHC (12Cr-1.6Co-1.5W) [15], typically used for direct steam generation, with a maximum field operating temperature around 600°C. The durability test procedure has been further updated, combining on-sun thermal tests, muffle furnace thermal tests and climate chamber tests. The analysis focuses on the degradation of opto-thermal figures of merit, i.e. the solar absorptance α_{sol} (%) and the thermal emittance ε_{th} (%).

MATERIALS AND METHODS

Solar Receiver Coatings

In this paper, six receiver coatings are compared:

a. A ceramic spray consisting of a primer coating and a HSA top coating (**Coating A**)
b. A slurry aluminide primer coating [16] protecting the steel substrate from hot oxidation, in combination with the above ceramic HSA top coating (**Coating B**)
c. A magnetron-sputtered multi-layered thin film cermet SSC applied on a polished substrate (**Coating C**)
d. A multi-metallic Cr-Mn diffusion coating [17] applied with the pack cementation process (**Coating D**)
e. A combination of the above slurry aluminide primer *(b)* with a thin film cermet SSC on top (**Coating E**)
f. A combination of the multi-metallic diffusion coating *(d)* as a primer coating combined with the ceramic HSA top coating *(a)* (**Coating F**)

Coatings A, B, C, D and E have been applied on T91 substrate, while coatings A, B, D and F have been applied on VM12. Table 1 summarizes some key specifications for the comparison of these coatings, dry film thickness (DFT), solar selectiveness (SSC), surface preparation, coating application, thermal treatment (curing). Solar selectiveness means a coating combining a high solar absorptance α_{sol} together with a low thermal emittance ε_{th}.

For combined testing, tubular samples with a 31.8 mm outer diameter, 5 mm wall thickness and 40 mm length are tested. For climate chamber tests, flat metal coupons with a 2 mm thickness of dimensions ranging from 30x30 mm^2 to 50x50mm^2 are tested.

TABLE 1. Description of solar receiver coatings. Coatings A, B, C and D are Gen 2 coatings, while coatings E and F are innovative hybrid coating formulations, each tested only on one of the substrate.
Nomenclature: DFT: Dry Film Thickness; SSC: Solar Selective Coating.

Coating	Substrate	Thickness (DFT, µm)	SSC	Surface preparation	Coating application	Thermal treatment
A	T91|VM12	~ 55	No	Grit blasting	Spraying	Curing
B	T91|VM12	85 | 55	No	Grit blasting	Spraying	Curing (x2)
C	T91	0.6	***Yes***	Polishing, mirror finish	Sputtering	-
D	T91|VM12	35	No	Glass bead blasting	Cementation	Pre-oxidation
E	T91	~ 65	No	Polishing	Spraying + Sputtering	-
F	VM12	~ 70	***Yes***	Glass bead blasting	Cementation + Spraying	Pre-oxidation + Curing

Optical Characterization

Spectral Reflectance Measurements

For each sample, the spectral hemispherical reflectance (SHR),[%] is measured at room temperature, for a wavelength ranging from 0.28 to 16 µm with two Perkin Elmer spectrophotometers. The SHR is measured first with the UV/Vis/NIR Lambda1050 spectrophotometer from 0.28 to 2.5 µm in steps of 5 nm, the incidence angle is 8°, the integrating sphere has a diameter of 150 mm, its interior is coated with Spectralon ($BaSO_4$, white diffuse), the measurement spot has a size of 9 x 17mm^2.

This SHR measurement is extended from 2.5 to 16 µm in steps of 4 nm with a Frontier Fourier Transform Infrared (FT-IR) spectrophotometer, the incidence angle is 12°, the integrating sphere has a diameter of 76.2 mm and its interior is coated with Infragold. The sample aperture has a diameter of 20 mm.

Both spectrophotometers overlap spectrally between 2.0 and 2.5 µm. The mismatch between both instruments, supposedly induced by different integration sphere diameters and detector types, is minimized by measuring calibrated baseline samples. Each coated sample is measured at three positions.

The analysis of spectra is further described in the next subsections. Reference spectra are shown in Fig. 1.a for calibrated sample coupons at OMT Solutions laboratory (traceable to NIST), while standard weighting spectra selected for the solar absorptance α_{sol} and thermal emittance ε_{th} calculations are shown in Fig 1.b.

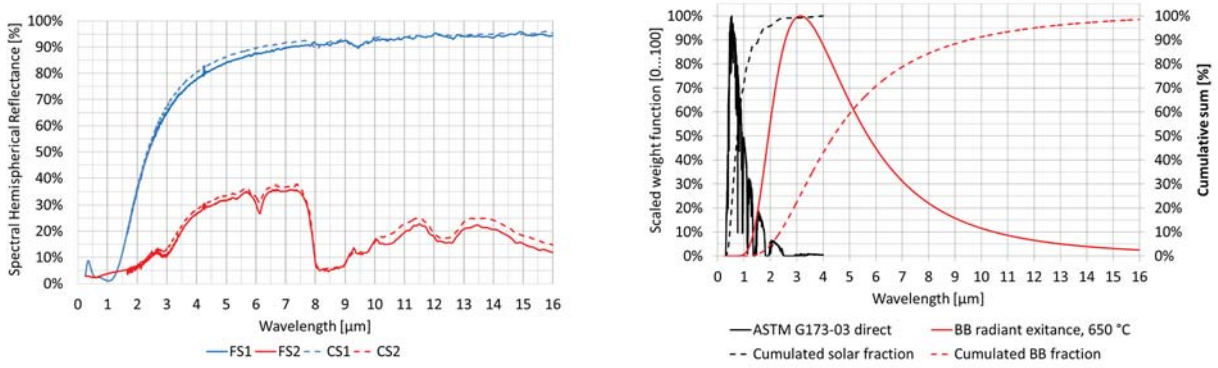

(a) Reference spectra for calibration coupons

(b) Weighting spectra

FIGURE 1. Reference (ref.) spectra for quantitative analysis. a) Calibrated coupons, FS1 is a flat SSC reference, FS2 is a flat black coating reference, CS1 is a curved SSC reference, CS2 is a curved black coating reference b) Weighting spectra, Solar Spectral Irradiance (ASTM G173-03, direct+circumsolar) and blackbody (BB) radiant exitance at 650 °C. The respective distributions are scaled with respect to their maximum. Cumulative fractions are shown in dotted line.

Spectral Quantitative Analysis

Processing of SHR data

For quantitative analysis, the SHR measurement is first processed according to (Eq.1):

$$\rho_{sample}(\lambda) = \frac{R_{sample,meas}(\lambda)}{R_{baseline,meas}(\lambda)} \rho_{baseline,ref}(\lambda) \tag{1}$$

where λ is the wavelength expressed in nm or µm, ρ_{sample} corresponds to the sample weighted SHR, $R_{sample,meas}$ is the SHR measurement data obtained for the sample, $R_{baseline,meas}$ is the SHR measurement data obtained for the selected baseline and $\rho_{baseline,ref}$ is the reference SHR for the selected baseline, calibrated by an external laboratory (Fig.1.a.). All quantities are expressed in %.

The rules for baseline selection are primarily based on geometry and spectral properties, i.e. one should select a baseline as similar as possible to the measured sample, with the same geometry and spectral properties. Otherwise, primary calibrated standards should be selected, i.e. Spectralon for the UV-VIS-NIR range or Infragold for the Mid Infrared (MIR) range. For the UV-VIS-NIR range, a black HSA coated baseline sample is used for all coatings. In the MIR range, a black HSA coated baseline is selected for coatings A, B, D and F and a SSC baseline is selected for coatings C and E.

Solar absorptance

The solar absorptance α_{sol} [%] is calculated according to (Eq.2):

$$\alpha_{sol}(AM) = \frac{\int_{\lambda_1}^{\lambda_2} [1-\rho_{sample}(\lambda)] G_{sol}(\lambda, AM) d\lambda}{\int_{\lambda_1}^{\lambda_2} G_{sol}(\lambda) d\lambda} \quad (2)$$

where AM is the Air Mass index, $G_{sol}(\lambda, AM)$ is the solar spectral irradiance shown in Fig.1.b). The reference spectrum is defined according to ASTM G173-03, AM1.5, direct+circumsolar. The wavelength ranges from λ_1 = 0.28 µm to λ_2=2.5 µm. As such, the Lambda1050 spectrophotometer delivers sufficient data for this calculation. It is worth noting that the denominator in (Eq.2) equals 900 W/m^2, 99% of which is radiated from 0.28 to 2.5 µm.

Thermal emittance

The thermal emittance ε_{th} [%] is calculated at a receiver temperature T [°C] according to (Eq.3) and (Eq.4):

$$\varepsilon_{th}(T) = \frac{\int_{\lambda_1}^{\lambda_3} [1-\rho_{sample}(\lambda)] M_{bb}(\lambda, T) d\lambda}{\int_{\lambda_1}^{\lambda_3} M_{bb}(\lambda, T) d\lambda} \quad (3)$$

$$M_{bb}(\lambda, T) = \frac{2\pi hc^2}{\lambda^5 [\exp(\frac{hc}{\lambda . k . T}) - 1]} \quad (4)$$

where M_{bb} is the blackbody spectral exitance in W/m^2.µm^{-1}, c,k and h are universal physical constants, which respectively correspond to the speed of light in vacuum (2.997 10^8 m.s^{-1}), Planck's constant (6.63 10^{-34} J.s) and Boltzmann's constant (1.38.10^{-23} J.K^{-1}). The wavelength ranges from λ_1 = 0.28 µm to λ_3=16 µm. As such, both spectrophotometers are required to measure the spectrum. For a blackbody radiating at 650 °C (Fig. 1.b), 12.4% of the radiation is emitted between 0.28 and 2.5 µm, while 98.5% of the radiation ($\sigma.T^4$) is emitted up to 16 µm.

Opto-thermal efficiency

The coating opto-thermal efficiency $\eta_{coating}$ [%] is calculated per surface unit according to (Eq.5):

$$\eta_{coating} \simeq \frac{\alpha_{sol} \dot{q}''_{sol} - \varepsilon_{th}(T_{abs}) \sigma T_{abs}^4}{\dot{q}''_{sol}} \quad (5)$$

where $\dot{q}''_{sol}$ is the incident solar flux density (W/m^2), T_{abs} is the absorber surface temperature (°C), and σ is the Stefan- Boltzmann constant (5.67 10-8 W.m^2.K^{-4}). This equation assumes a flat geometry for the absorber, radiating to an infinite heat sink at 0K in a perfect vacuum. This simple equation allows isolating the contribution of the coating opto-thermal performance, combining into a single performance criterion the solar absorptance α_{sol} and the thermal emittance ε_{th}. (Eq.5) allows the definition of a trade-off factor Z between both performance indicators, with respect to the local operating point $\{T_{abs}, \dot{q}''_{sol}\}$, as described in (Eq. 6):

$$Z = \frac{\Delta \alpha_{sol}}{\Delta \varepsilon_{th}} = -\frac{\dot{q}''_{sol}}{\sigma T_{abs}^4} \quad (6)$$

According to (Eq. 6), for any operating point $\{T_{abs}, \dot{q}''_{sol}\}$, increasing the α_{sol} value by 1% yields a 1% increase in opto-thermal efficiency $\eta_{coating}$. Assuming a flux density of 250 kW/m^2 and a surface temperature of 650 °C for the dish test presented further, increasing the α_{sol} *value* by 1% has the same impact on $\eta_{coating}$ as reducing the ε_{th} value by -6.1%. These operating conditions favor stable selective coatings in terms of opto-thermal efficiency. However these are not representative of the receiver operation, given the Allowable Flux Density (AFD) constraint [18]. At high flux (1000 kW/m^2) and low temperature (300°C), increasing the α_{sol} value by 1% would have the same impact on the opto-thermal efficiency $\eta_{coating}$ as reducing the ε_{th} value by roughly -150%.

As such, the α_{sol} value is considered as a dominant performance factor for further analysis. As shown in [11], an oxidized bare VM12 substrate already reaches an α_{sol} value of 92-94%. HSA coatings should have an α_{sol} value above 96%. One failure criterion defined in the literature [9] sets a threshold α_{sol} value of 95% for recoating.

Visual Inspection

In addition to discrete spectral measurements, sample imaging is performed with a Panasonic DMC FZ45 digital camera and a Zeiss Axio CSM 700 microscope to monitor respectively millimetric and microscopic surface defects, such as corrosion spots, delamination or cracks, which are not necessarily detected by both spectrophotometers.

Durability Testing

The receiver coating durability test program carried out within the Raiselife project includes:

- Muffle furnace testing: Isothermal and cyclic thermal loads
  - Isothermal testing: 2000 hours exposure at 600, 620 and 650 °C
  - Cyclic thermal loads: 200 cycles from 200 to 650°C, 30 min dwell time, ~ 25 min ramps
- On-sun testing with thermal cycling and concentrated solar radiation
  - Slow cycling ramps from 200 to 650 °C, max. 30 K/min, isothermal stage at 650 °C for 30 minutes [11], 100 cycles
  - Fast cycling ramps to reproduce fast transients due to cloud passage [12]
- Climate chamber tests for environmental conditions

Muffle furnace testing allow the evaluation of coating degradation under laboratory conditions, isolating temperature levels and gradients without applying solar radiation. On-sun testing allows reproducing realistic field conditions, both outdoor at a DISTAL II dish test facility located at the Plataforma Solar de Almeria, Spain (CIEMAT-PSA) [11] and indoor at the SAAF facility in Odeillo, France (CNRS-PROMES) [12]. Both tests require suitable meteorological test conditions, at least a Direct Normal Irradiance (DNI) 700 W/m2. This paper focuses on the results of outdoor slow-cycling on-sun testing.

Climate chamber tests allow performing standard environmental testing, in order to assess coating degradation when the receiver is not in operation (simulating night-time or down-time due to maintenance). In order to predict service lifetime, one would have to correlate these test conditions with meteorological data (sand storm events, corrosivity class, ambient temperature, humidity) for relevant test sites.

Combined Testing

The outdoor on-sun testing has been previously described in [11]. This test has been extended with an isothermal muffle furnace test and a 100 hours condensation test according to ISO 6270 [11], i.e. 40 °C ambient temperature and 100% relative humidity. The test sequence is shown in Fig. 2. Optical characterization is carried out after each test and every 25 dish cycles. This test is performed on 15 tubular samples, irradiated on one side during solar cycling. Samples are exposed to outdoor conditions during night, allowing exposure to potential soiling events.

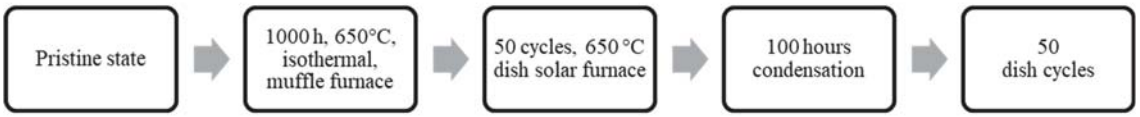

FIGURE 2. Description of the combined test sequence including outdoor on-sun testing.

It is worth remarking that the 650 °C temperature setpoint is 50 °C above the nominal operating temperature. The heating and cooling rates are set to 30 °C/min and are three times faster than normal operation. The average flux density on the receiver panel is allowed to vary from 40 kW/m^2 to 250 kW/m^2, in order to maintain linear temperature ramps using air cooling.

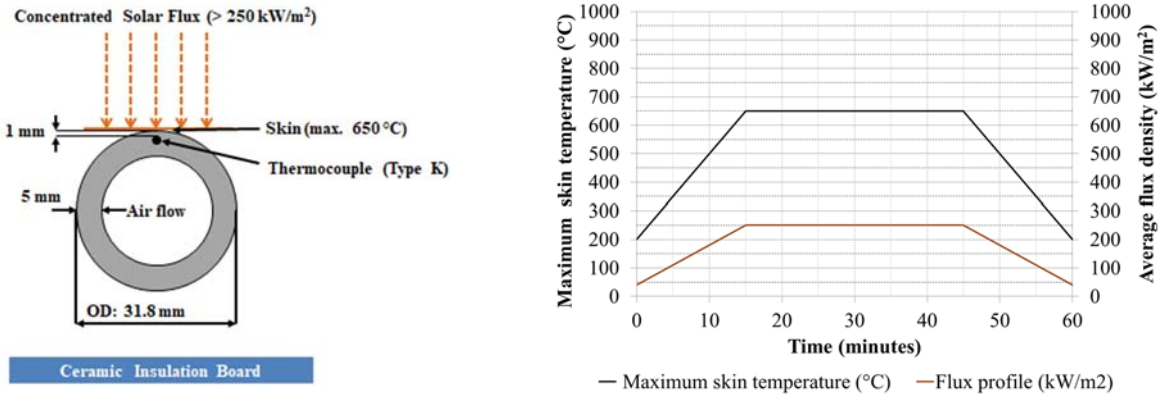

(a) Sample cross-section with thermocouple.

(b) Test cycle definition (skin temperature and flux density).

FIGURE 3. Description of the combined test sequence including outdoor on sun testing.

Climate Chamber Tests

Climate chamber tests are listed in Table 2. Four climate chamber tests are performed: a) Damp Heat (DH), b) Humidity Freeze (HF), c) Neutral Salt Spray (NSS) and d) Sand Erosion (SE). For each coating, three flat coated samples are exposed in the corresponding climate test chamber. The NSS test is interrupted after 120 hours to discard severely corroded samples and resumed until 480 hours.

TABLE 2. Summary of climate chamber test conditions.

Test	DH	HF	NSS	SE
Standard	IEC 62108, Test 10.7b	IEC 62108, Test 10.8	ISO 92237	Based on MIL-STD 810 G
Duration	1000 hours	1500 hours	120, 480 hours	-
Parameters	T_{amb}: 65 °C RH: 85 %	T_{amb}: -40 to 65 °C RH: max. 85%	T_{amb}: 35 °C pH 6.5 to 7.2 at 25 °C	20 m/s; 3x 70 g std blowing dust

RESULTS AND DISCUSSION

Pristine State

Initial α_{sol} and ε_{th} (650°C) values are reported in Table 3 for all coatings in pristine state, before durability testing. For each coating, the statistics is derived for a batch of 12 flat coated samples and 3 coated tube samples. By definition, a SSC absorbs a maximum amount of solar radiation (high α_{sol} value) and emits a minimum of thermal radiation (low ε_{th} value).

One can first observe that coatings A, B, E and F achieve a α_{sol} value above 96% in pristine state. These coatings thus can be qualified as HSA. Coating C achieves the α_{sol} HSA target for tube samples but not for flat samples. Coating D does not achieve the minimal requirement for α_{sol} value of 95%. It brings marginal benefit in comparison with an oxidized bare substrate.

Calculated values for ε_{th} (650°C) achieve lower levels for SSC formulations (Coatings C and E). Coating C almost achieves the theoretical minimal thermal emittance for a selective coating with a cut-off wavelength (SHR = 50%, Fig. 1.a) of 2.5 µm, given the overlap between the solar spectrum and the blackbody spectrum, shifting towards lower wavelengths at higher temperature because of Wien's displacement law. Coating E is less selective than Coating C and emits 10% more thermal radiation. Coatings A, B and F exhibit similar spectral properties and are only "mildly" selective, while Coating D behaves nearly as a grey body.

Before durability testing, Coating E could be considered as the most promising candidate in terms of efficiency, as it combines both the HSA and SSC features, albeit its application cost remain unknown, in contrast to Coating A, which corresponds to a commercial product applied at Ivanpah Solar Thermal Power Plant.

TABLE 3. Summary of α_{sol} and ε_{th} (650°C) values for all coatings in pristine state.

Coating	T91 - Tube	VM12 - Tube	T91 - Flat	VM12 - Flat
Coating A	α_{sol} = 96.4 ±0.1% ε_{th} = 79.0 ± 0.6%	α_{sol} = 96.0 ±0.1% ε_{th} = 77.0 ± 0.2 %	α_{sol} = 96.4 ± 0.1% ε_{th} = 78.4 ± 0.4%	α_{sol} = 96.2 ± 0.1% ε_{th} = 76.4 ± 0.7 %
Coating B	α_{sol} = 96.5 ± 0.1% ε_{th} = 76.5 ± 0.3%	α_{sol} = 96.1 ± 0.1% ε_{th} = 77.0 ± 0.2%	α_{sol} = 96.6 ± 0.2% ε_{th} = 76.0 ± 0.6 %	α_{sol} = 96.2 ± 0.1% ε_{th} = 77.2 ± 0.5%
Coating C	α_{sol} = 96.2 ± 0.2% ε_{th} = 29.3 ± 1.2%	Not applied	α_{sol} = 94.9 ± 0.6% ε_{th} = 26.8 ± 0.3%	Not applied
Coating D	α_{sol} = 94.5 ± 0.1% ε_{th} =85.0 ± 0.3%	α_{sol} = 94.5 ± 0.2% ε_{th} = 85.3 ± 0.1%	α_{sol} = 94.6 ± 0.1% ε_{th} = 85.9 ± 0.3%	α_{sol} = 94.7 ± 0.1% ε_{th} = 84.8 ± 0.5%
Coating E	α_{sol} = 96.4 ± 0.1% ε_{th} = 43.1 ± 0.3%	Not applied	α_{sol} = 96.2 ± 0.1% ε_{th} = 41.6 ± 0.3%	Not applied
Coating F	Not applied	α_{sol} = 96.4 ± 0.1% ε_{th} = 76.6 ± 1.4%	Not applied	α_{sol} = 96.8 ± 0.1% ε_{th} = 78.9 ± 0.6%

Combined Testing

Optical characterization results during the combined testing are plotted in Fig. 4-5 for all substrates and coatings.

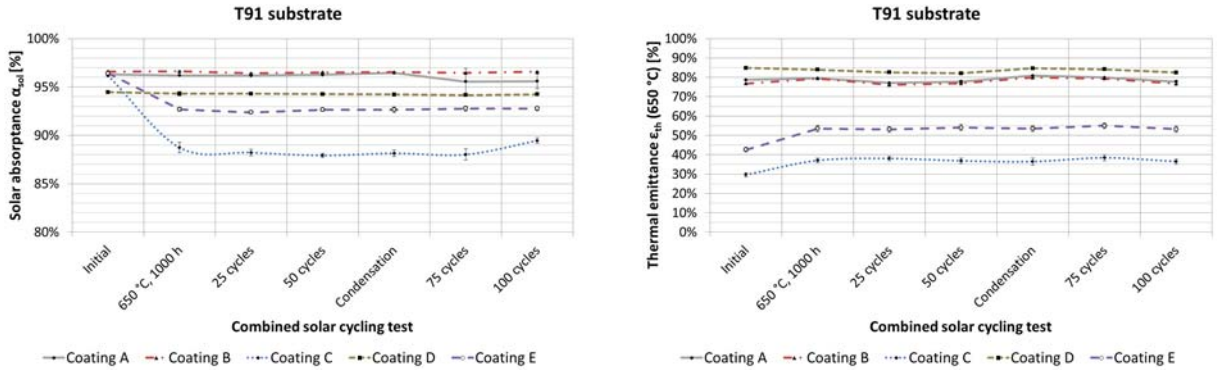

a) Combined solar cycling test, T91 substrate, α_{sol}

b) Combined solar cycling test, T91 substrate, ε_{th} (650°C)

FIGURE 4. Optical characterization results during combined solar cycling test.
a) T91 substrate, solar absorptance α_{sol} b) T91 substrate, thermal emittance ε_{th} calculated at 650 °C.

On T91 substrate, Coating A remains stable until after the condensation test, where one of the two exposed sample starts peeling locally, inducing a drop in the α_{sol} value, while the other sample exposed to similar conditions remains optically stable. Coating B remains optically stable, while microscopic oxidation dots start propagating after 100 dish cycles. Coating C exhibits a significant drop in the α_{sol} value (- 7 p.p.) after the isothermal furnace test at (650 °C, 1000 hours). Its ε_{th} value also increases by +7 p.p. After 100 dish cycles the α_{sol} value raises up to 90% as the substrate starts oxidizing. Coating D remains optically stable throughout testing, without noticeable visual degradation. Finally, Coating E also exhibits optical fading, i.e. a drop in the α_{sol} value of -3.5 p.p. and the ε_{th} value increases by +11 p.p. after the isothermal furnace test (650 °C, 1000 hours).

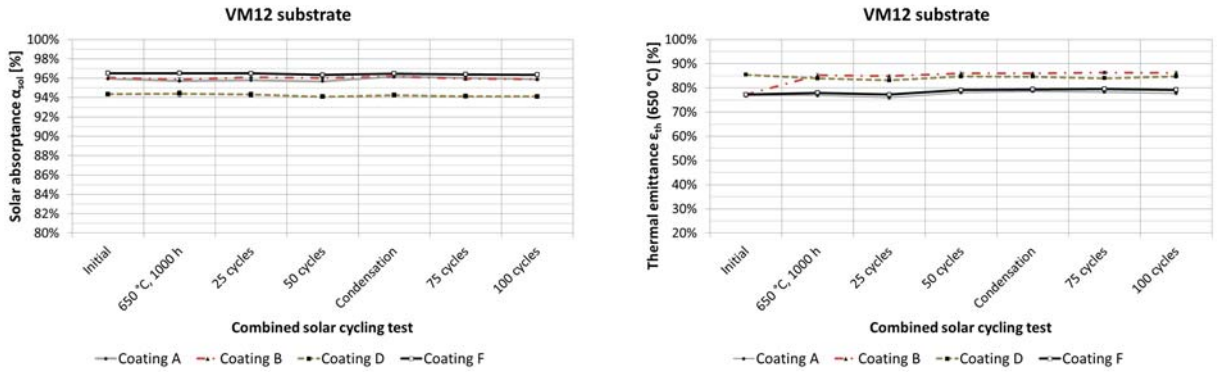

a) Combined solar cycling test, VM12 substrate, α_{sol}

b) Combined solar cycling test, VM12 substrate, ε_{th} (650°C)

FIGURE 5. Optical characterization results during combined solar cycling test.
a) VM12 substrate, solar absorptance α_{sol}, d) VM12 substrate, thermal emittance ε_{th} calculated at 650 °C.

On VM12 substrate, Coating A remains optically stable throughout testing, although local peeling and micro-cracks start to be observed, especially on sample edges. Coating B initial thickness (DFT) looks initially inhomogeneous. This coating degrades after isothermal testing (650 °C, 1000 hours), the top coat disappears on the lower section, where the slurry aluminide layer and the bare oxidized substrate appear. While the α_{sol} value remains constant at the measured spots, the ε_{th} value increases by +8 p.p., from 77% to 85%. Coating D remains optically stable, although light scratches from sample mounting induce a minor drop in the α_{sol} value (-0.3 p.p.). Coating F also remains optically stable, although microscopic oxidation spots start to appear after 100 dish cycles.

To summarize, degradation is observed on most of the coatings during the combined solary cycling test procedure. Adhesion issues are observed for coating A on both substrates. Oxidation spots start to appear on Coating B (T91) and Coating F (VM12). Coating B (VM12) degrades after the isothermal test, while solar selective coatings (Coating C and E) fail this test. Coating D remains optically stable, however this coating did not achieve the solar absorptance target and exfoliation is observed during testing.

Climate Chamber Tests

Optical characterization results after climate chamber tests are plotted in Fig. 6-7 for all substrates and coatings. Globally, it is worth remarking that optical degradation can be observed for some coatings when observing α_{sol} values, while ε_{th} (650°C) values remain stable. Most of the coatings pass the DH and HF tests, while more pronounced degradation can be observed after NSS and SE tests.

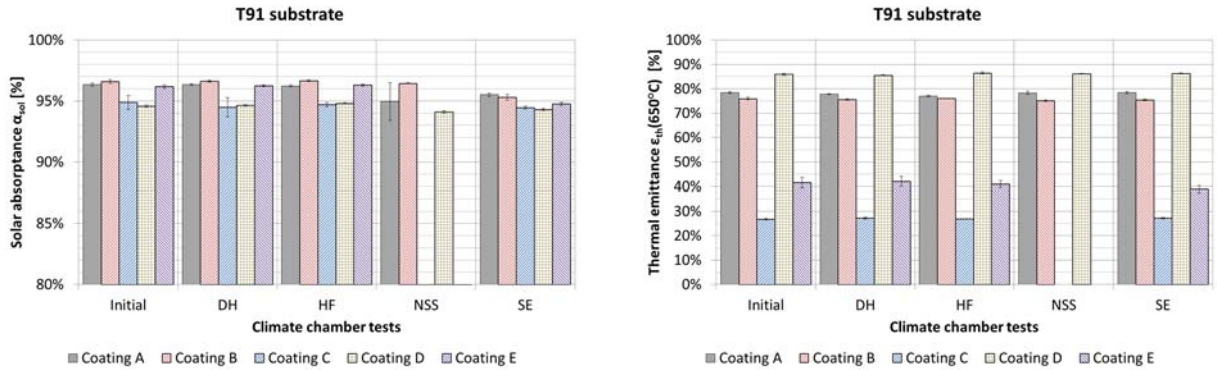

(a) Climate chamber test, T91 substrate, α_{sol}

(b) Climate chamber tests, T91 substrate, ε_{th} (650°C)

FIGURE 6. Optical characterization results after climate chamber tests.
a) T91 substrate, solar absorptance α_{sol}, b) T91 substrate, thermal emittance ε_{th} calculated at 650 °C.

On T91, Coating A remains optically stable after DH and HF tests. Corrosion is however observed after NSS test and optical fading is observed after SE test ($\Delta\alpha_{sol,SE}$ = -0.9 p.p., $\alpha_{sol,SE}$ = 95.5%). Coating B also remains optically stable after DH and HF tests and it resists better to the NSS test, although edge corrosion is observed. This coating also shows optical fading after the SE test ($\Delta\alpha_{sol,SE}$ = -1.3 p.p., $\alpha_{sol,SE}$ = 95.3%). Coating C also passes DH and HF tests, but it fails the NSS test and is removed after 120 hours. Nonetheless, it does not degrade after the SE test. Coating D passes the DH and HF tests. It degrades moderately after the NSS test and it does not degrade after the SE test. Coating E passes the DH and HF tests, while it fails the NSS test after 120 hours due to severe corrosion. This coating fades optically after the SE test ($\Delta\alpha_{sol,SE}$ = -0.8 p.p.) but keeps its HSA feature ($\alpha_{sol,SE}$ = 96%).

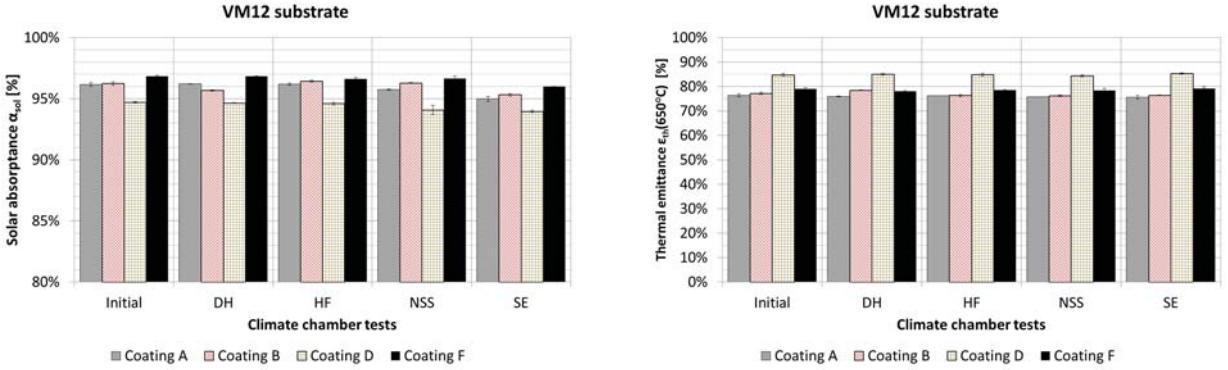

a) Climate chamber tests, VM12 substrate, α_{sol}

(d) Climate chamber tests, VM12 substrate, ε_{th} (650°C)

FIGURE 7. Optical characterization results after climate chamber tests.
a) VM12 substrate, solar absorptance α_{sol}, b) VM12 substrate, thermal emittance ε_{th} calculated at 650 °C.

On VM12, Coating A nearly behaves as on T91. It passes DH and HF tests, some edge corrosion is observed after NSS test ($\Delta\alpha_{sol,NSS}$ = -0.5 p.p., $\alpha_{sol,NSS}$ = 95.7%) and optical fading is observed after SE test ($\Delta\alpha_{sol,SE}$ = -1.2 p.p., $\alpha_{sol,SE}$ = 95.0%). Coating B degrades after DH test ($\Delta\alpha_{sol,DH}$ = -0.5 p.p., $\alpha_{sol,SE}$ = 95.7%), it passes the HF and NSS test, while it fades after the SE test ($\Delta\alpha_{sol,SE}$ = -0.9 p.p., $\alpha_{sol,SE}$ = 95.3 %). Coating D passes the DH and HF test, it degrades moderately after the NSS and SE tests ($\Delta\alpha_{sol,NSS/SE}$ = -0.7 p.p., $\alpha_{sol,NSS} = \alpha_{sol,\ SE}$ = 94.0%). Coating F passes the DH and HF test, its solar absorptance remains constant after NSS test, although corrosion is observed locally. Finally, it fades after the SE test ($\Delta\alpha_{sol,SE}$ = -0.8 p.p.) but keeps its HSA feature ($\alpha_{sol,SE}$ = 96%).

To summarize, none of the tested coating pass all climate chamber tests. Even if the optical figures of merit remain stable, visual degradation can be observed on several samples. Both SSC formulations (Coatings C and E) fail the NSS test after 120 hours. All other coatings fade after the SE test. Coating B appears as the most stable coating after climate chamber tests. Detailed real environmental conditions for salinity and sandstorm events applicable for solar tower receivers mounted at a height above 200 meters remain unknown, Service Lifetime Prediction (SLP) remains a challenging task and the severity of applied test conditions cannot be determined properly yet.

CONCLUSION

In this paper, six different receiver coatings applied on T91 and VM12 substrates were compared with respect to their opto-thermal performance. The durability test program included on the one hand a combined test, sequencing a muffle furnace isothermal test at 650°C for 1000 hours, thermal cyclic loads under concentrated solar radiation (300 kW/m^2) for 50 hours at a dish concentrator, a 100 hours condensation test and another 50 hours of on-sun testing in the dish concentrator. On the other hand, standard climate chamber tests were performed on all coatings to assess their durability under environmental loads.

The durability test program showed to be more aggressive in comparison to the first generation. Few of the tested coatings remained optically stable, i.e. without observing any visual degradation or solar absorptance drop. Solar selective coatings failed both the isothermal muffle furnace test and the Neutral Salt Spray test. Coatings D did not reach the initial solar absorptance target and brings marginal improvement in comparison to a bare oxidized substrate. Coatings B applied on T91 and coating F applied on VM12 could be the most relevant, if salinity levels and sandstorm events are not critical at the power plant site.

Metallurgical analysis of all tested samples will be conducted. Isothermal and cyclic thermal muffle furnace tests are currently in progress for these coatings. Experimental data will be compared with on-sun testing to develop service lifetime prediction models. So far, only marginal improvements could be noticed in comparison to the first coating generation. The durability test program is currently applied on austenitic Nickel-Chromium superalloys, such as Inconel 617 and Haynes 230. After climate chamber tests, Inc617 and H230 samples show a better resistance to Neutral Salt Spray and Sand Erosion test conditions.

ACKNOWLEDGMENTS

Financial support from the European Union is gratefully acknowledged (EU-Raiselife project, Horizon 2020, Contract n°686008). The main author thanks Vallourec for supplying T91 and VM12 substrates, laboratory technicians, all involved project partners for suppling coated samples, Lucia Martinez, Carmen Amador and Tomas Reche for their technical assistance in optical measurements and climate chamber tests, David Muruve and Jose Galindo for the maintenance of the dish test bench, sample preparation and mounting.

REFERENCES

1. C.K. Ho et al., "Characterization of High-Temperature Solar Receivers", *Journal Solar Energy Engineering*, **136**, 041502-1:4 (2014).
2. A. Ambrosini et al., " Influence of application parameters on stability of Pyromark® 2500 receiver coating", *AIP Conference Proceedings*, **2126**, 030002 (2019).
3. I. Jerman et al., "Merging of oxide species with black spinel structure by CSP operating temperature", *AIP Conference Proceedings*, **2033**, 220002 (2018).
4. K. Tsuda et al., "Development of high absorption, high durability coatings for solar receivers in CSP plants", *AIP Conference Proceedings*, **2033**, 040039 (2018).
5. R. Harzallah et al., "Development of high performances solar absorber coatings", *AIP Conference Proceedings*, **2126**, 030026 (2019).
6. C. K. Jo, J. Pacheco, "Levelized Cost of Coating (LCOC) for selective absorber materials", *Solar Energy*, **108**, 315-321 (2014).
7. A. Boubault et al., "Durability of solar absorber coatings and their cost-effectiveness", *Solar Energy Materials & Solar Cells*, **166**, 176-184 (2017).
8. J. F. Torres et al., "Effects of Cyclic Thermal Ageing on Coating Degradation", presented at SolarPACES 2018 Conference, Casablanca, Morocco, 2-5th October, (2018).
9. L. Noč et al., "High-solar-absorptance CSP coating characterization and reliability testing with isothermal and cyclic loads for service-life prediction", *Energy & Environ. Sci.*, **12**, 1679-1694, (2019).
10. Raiselife EU project, Horizon 2020, https://www.raiselife.eu/
11. S. Caron et al., "Accelerated ageing of solar receiver coatings: Experimental results for T91 and VM12 steel substrates", *AIP Conference Proceedings*, **2033**, 230002 (2018).
12. R. Reoyo-Prats et al., "Accelerated aging of absorber coatings for CSP receivers under real high solar flux – Evolution of their optical properties", *Solar Energy and Material Cells*, **193**, 92-100, (2019).
13. C.K. Ho, "Advances in central receivers for concentrating solar applications", *Solar Energy*, **152**, 38-56 (2017).
14. T91/P91 short description, http://www.vallourec.com/fossilpower/EN/Products/Pages/tp91.aspx
15. VM12-SHC short description, http://www.vallourec.com/fossilpower/EN/Products/Pages/vm12-shc.aspx
16. A. Agüero et al., "Deposition process of slurry iron aluminide coatings", *Materials at High Temperature*, Vol. **25**, Issue (4), 257-265 (2008).
17. T. Meissner et al., "Improving optical properties of diffusion based absorber coatings for CSP tower systems", *AIP Conference Proceedings*, **2126**, 020003 (2019).
18. L.L. Vant-Hull, "The Role of "Allowable Flux Density" in the Design and Operation of Molten Salt Solar Central Receivers", Journal of Solar Energy Engineering, **124**, 165-169, (2002).